

Full Length Article

Improving the catalytic performance of Ag/SiC for ethylene epoxidation via modifying SiC surface using CeO₂

Xiang Li ^{a,b}, Jixiao Zhao ^{b,*}, Zhenni Wei ^c, Xiaofei Liu ^c, Xin Huang ^c, Guoqiang Zhang ^c, Yu Liu ^b, Zhifeng Jiao ^b, Xiangyun Guo ^{b,*}

^a School of Materials Science and Engineering, Changzhou University, Changzhou 213164 Jiangsu, China

^b Jiangsu Key Laboratory of Advanced Catalytic Materials and Technology, School of Petrochemical Engineering, Changzhou University, Changzhou 213164 Jiangsu, China

^c Lanzhou Petrochemical Research Center, Petrochemical Research Institute, Petro China Co., Ltd, Lanzhou 730060, China

ARTICLE INFO

Keywords:

Ethylene epoxidation
SiC support
CeO₂ modification
Reactive oxygen species
Oxygen migration

ABSTRACT

Ethylene epoxidation over high-loading Ag/α-Al₂O₃ catalysts is an important industrial process to produce ethylene oxide. However, the low specific surface area and poor thermal conductivity of α-Al₂O₃ restrict further improvement of the catalyst's performance in ethylene epoxidation. In this work, we employed CeO₂-modified SiC as the support of active component Ag for the ethylene epoxidation reaction. Under the condition of 230 °C, 2 MPa, gas hourly space velocity of 3540 h⁻¹, the catalyst achieved good performance without any additives. The conversion, ethylene oxide selectivity, and space-time yields were 5.4 %, 74.3 %, and 66 kg/(m³·h), respectively. The experimental and calculation results showed that oxygen molecules were activated on the Ag catalyst surface to form ¹O₂ and •O₂ species. These species then migrated onto the SiC with the ethylene adsorbed on the SiC surface. The oxygen vacancies in CeO₂ promote the migration of these oxygen species, and thus enhance the reaction performance.

1. Introduction

Ethylene oxide (EO) is an important chemical feedstock and organic intermediate, with an annual production exceeding 37 million tons [1]. In industry, EO is widely used to produce a variety of chemicals, including ethylene glycols, glycol ethers, and ethanol amines. Traditionally, EO was mainly produced through the chlorohydrin method. However, this method has serious pollution issues and has been eliminated. Currently, EO is primarily produced through green and environmentally friendly direct oxidation method [2]. Ag is the most commonly used catalytic metal for ethylene epoxidation due to its ability to effectively activate O₂ [3]. The advantage of Ag is that oxygen can form various oxygen species on its surface without causing complete combustion of ethylene, which is beneficial to the production of EO. Transition metals are usually prone to activate C–H bonds and thus leading to the formation of combustion products [4]. This is the difference between Ag and transition metals [5,6].

In industry, Ag/α-Al₂O₃ catalysts are commonly used for the production of EO. Typically, the specific surface area of α-Al₂O₃ support is

very low, and the silver loading on the α-Al₂O₃ is as high as 15–30 % by weight [7]. Since the EO selectivity of the pure Ag catalyst is approximately 50 % [3,8], it is necessary to add alkali metals or oxygen-containing anions to enhance the selectivity in practical applications [9,10]. Although Ag/α-Al₂O₃ catalysts have been used in the industrial production of EO, the studies on improving Ag catalysts have never stopped. Many efforts have been dedicated to improving the catalysts by reducing Ag content, adding additives, and modifying the carrier [10–13]. Van Hoof et al. prepared Ag/α-Al₂O₃ catalysts by adjusting the amount of silver oxalate during impregnation. Among these catalysts, Ag/α-Al₂O₃ catalysts with Ag contents of 5 wt% and 10 wt% achieved EO selectivities of 50 % and 75 %, respectively [14]. Additionally, they found that chlorine could break up Ag particles with a particle size exceeding 100 nm and redistribute active silver particles. Ren et al. prepared an Ag catalyst with an Ag content of 15 wt% and modified it with Cs and Re. The catalyst achieved an EO selectivity of approximately 83.5 %. The authors suggested that the synergistic electronic effect between Cs and Re was key to promoting the formation of weakly adsorbed oxygen species and enhancing the EO selectivity [15].

* Corresponding authors.

E-mail addresses: zhaojixiao@cczu.edu.cn (J. Zhao), xyguo@cczu.edu.cn (X. Guo).

The low specific surface area of $\alpha\text{-Al}_2\text{O}_3$ easily leads to poor dispersibility of Ag [16]. Typically, achieving high EO selectivity requires sacrificing ethylene conversion, which results in lower yields of ethylene oxide [17]. Therefore, many researchers were committed to designing new catalytic systems. For example, MnO_2 , SrFeO_3 , TiO_2 , and CuO were used as catalyst supports [12,16,18,19]. However, the ethylene epoxidation reaction is a strongly exothermic process, accompanied by two side reactions: the combustion of ethylene oxide and the combustion of ethylene [20]. More importantly, oxide carriers are prone to thermal agglomeration and deactivation of active metals due to their low thermal conductivity [21]. Therefore, it is essential to consider both the specific surface area and the thermal conductivity of the carrier material when designing catalyst systems.

$\beta\text{-SiC}$ is a kind of semiconductor materials with excellent electrical and thermal conductivity, and has been successfully used as the catalyst carrier for various catalytic reactions [22]. Meanwhile, its high specific surface area can improve the dispersibility of active metals. Previous studies have found that SiC can serve not only as a carrier of active metals but also as an active surface for adsorbing and activating some reactants, such as nitroarenes, nitriles, cinnamaldehyde and styrene [23–27]. In the Ag/SiC-catalyzed epoxidation of styrene, the SiC support adsorbed styrene and activated the C=C in the molecule. Then the adsorbed styrene and spillover of active oxygen species reacted on the SiC surface [27]. SiC as the catalyst support can provide abundant active sites for reactions, thereby exhibiting enhanced catalytic performance. CeO_2 owns plenty of oxygen vacancies due to the different valence states of Ce [28], and these oxygen vacancies can promote the migration of oxygen species and increase oxygen storage capacity [29], thus enhance the performance of oxygen-contained reactions.

In this work, we employed SiC with high specific surface area as the carrier to disperse 15 wt% Ag for ethylene epoxidation. The results showed that the selectivity of EO reached over 70 % but the ethylene conversion was very low. By modifying the SiC with CeO_2 , the conversion was significantly increased from 0.7 % to 5.4 % while the EO selectivity maintained beyond 70 %. Further investigations revealed that the CeO_2 modification effectively increased the concentration of reactive oxygen species, and thus improved the catalytic activity.

2. Experiment

2.1. Catalyst preparation

Powder $\beta\text{-SiC}$ carrier with a specific surface area of $68 \text{ m}^2/\text{g}$ was commercially purchased from ReginTech. Before the experiment, SiC powder was purified in a mixture composed of HF and HCl to remove any possible impurities. After the washing, the powders were rinsed until neutral and dried. The CeO_2 modification was described as follows. 1.9 g washed SiC was dispersed in 50 mL anhydrous ethanol, followed by addition of the $\text{Ce}(\text{NO}_3)_3 \cdot 6\text{H}_2\text{O}$ solution (0.116 M). After stirring for 3 h, the ethanol and water in the mixture were removed by vacuum rotary evaporation. Subsequently, heat treatment was carried out in a muffle furnace at 500°C for 4 h. The obtained sample was named as 5 % $\text{CeO}_2\text{-SiC}$, in which the CeO_2 modification amount was 5 wt%. Similarly, different CeO_2 -modified carriers were prepared by varying the amount of $\text{Ce}(\text{NO}_3)_3 \cdot 6\text{H}_2\text{O}$, and named as $x\%\text{CeO}_2\text{-SiC}$ ($x = 3, 5, 7, 10$). The Ag/ $\text{CeO}_2\text{-SiC}$ catalysts with 15 wt% Ag loading were prepared by the method reported previously [27], and the catalysts were named Ag/ $x\%\text{CeO}_2\text{-SiC}$ ($x = 3, 5, 7, 10$).

2.2. Catalyst test

The reaction was carried out in a tubular fixed bed reactor (i.d. = 6 mm) with a length of 200 mm. The Ag/ $x\%\text{CeO}_2\text{-SiC}$ catalyst was shaped into tablets and subsequently crushed into 10–20 mesh particles. 2 mL of the formed catalyst was placed into the reactor for the reaction. The packing density of Ag/ $x\%\text{CeO}_2\text{-SiC}$ catalyst was $\sim 1.15 \text{ g/cm}^3$. Firstly,

the reactor bed was heated to 200°C in an N_2 atmosphere. Subsequently, the reactor was slowly heated at a rate of $1^\circ\text{C}/\text{h}$ to activate the catalyst, and the temperature was finally raised to the reaction temperature of 230°C . Next, the mass flow controller was gradually adjusted until the proportions of ethylene, oxygen, and N_2 in the reaction gas were 28.3 vol%, 7.6 vol%, and 64.1 vol%, respectively. The gas hourly space velocity (GHSV) of the reactant gas was 3540 h^{-1} . The ethylene epoxidation reaction was performed at 230°C and 2 MPa. The reaction products were detected using online gas chromatography-mass spectrometry (Thermo Scientific, Prima PRO). The ethylene conversion, EO selectivity, and space-time yield were calculated using formulas (1)–(3):

$$\text{Conversion} = \frac{\text{Initial mole number} - \text{Final mole number}}{\text{Initial mole number}} \times 100\% \quad (1)$$

$$\text{EO Selectivity} = \frac{\text{EO mole number of product}}{\text{mole number of all products}} \times 100\% \quad (2)$$

$$\text{EO space-time yield} = \frac{\text{GHSV} \times \Delta C \times M_{\text{EO}}}{100 \times V_{\text{molar}}} \quad (3)$$

where ΔC is the EO concentration difference between the outlet and the inlet, M_{EO} is the molar mass of EO, and V_{molar} is the volume of 1 mol gas under standard conditions.

The details for catalyst characterization and other experiments were described in supporting information.

3. Results and discussions

The actual Ag content measured by titration was approximately 14.4 % (Table S1), closely matching the theoretical value of 15 wt%. Fig. 1 showed the reaction performances of different catalysts for ethylene epoxidation. From the figure, the ethylene conversion and EO selectivity of unmodified Ag/SiC were 0.7 % and 70 %, respectively. Although the selectivity was higher than those reported of pure Ag catalysts [3,8], the conversion rate was very low. The CeO_2 modification significantly improved the conversion. As the amount of CeO_2 modification increased, the catalytic performance exhibited a volcano-shaped curve. When the CeO_2 modification amount was 5 wt%, the ethylene conversion and EO selectivity reached the highest values, 5.4 % and 74.3 % respectively. Correspondingly, the space-time yield was $66 \text{ kg}/(\text{m}^3 \cdot \text{h})$. The effect of CeO_2 modification on the catalytic performance shows a double-edged sword effect. The conversion rate of ethylene was significantly enhanced at low levels of CeO_2 modification. However, excessive

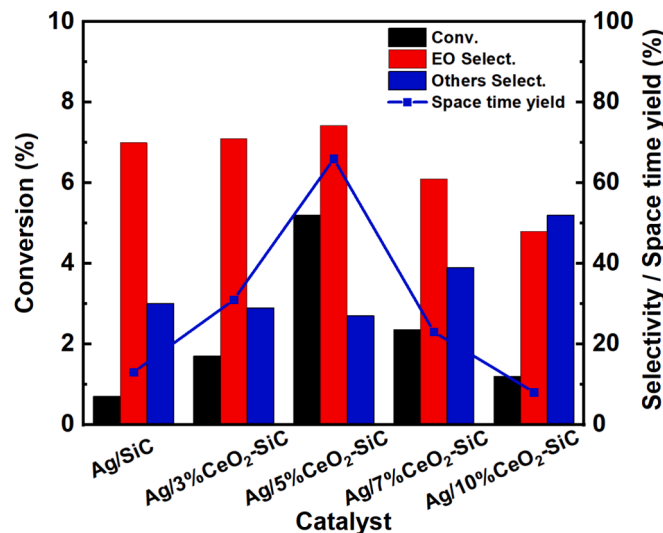


Fig. 1. Catalytic performances of Ag catalysts supported by the SiC modified with different amount of CeO_2 .

CeO_2 modification leads to a decrease in the ethylene conversion rate and an increase in by-products (such as H_2O and CO_2). Therefore, the optimal CeO_2 modification amount was 5 wt%. Moreover, the catalyst exhibited good stability (Fig. S1).

Compared with the performance of industrial and reported $\text{Ag}/\text{Al}_2\text{O}_3$ catalysts, Ag/SiC -based catalysts exhibit lower ethylene epoxidation performance (Table S2). This may be due to the fact that the good performance of $\text{Ag}/\text{Al}_2\text{O}_3$ catalysts typically requires promoters such as Cl, Re, Cs, etc. Without these promoters, the EO selectivity is only around 50 % [30]. In contrast, in our work, the EO selectivity over Ag/SiC base catalysts can exceed 70 % without promoters, showing a significant advantage over $\text{Ag}/\alpha\text{-Al}_2\text{O}_3$ catalysts.

The catalysts were characterized using XRD and TEM tests. The XRD results indicate that the catalyst contains Ag and CeO_2 . The peak intensity of CeO_2 increases with the increasing amount of CeO_2 modification. Since all catalysts have an Ag content of 15 wt%, there is no significant difference in the peaks of Ag (Fig. S2). Fig. 2(a-d) show the TEM images of Ag/SiC and $\text{Ag}/5\%\text{CeO}_2\text{-SiC}$ catalysts. From these images, the Ag particles over the both supports have relatively uniform distribution. In Fig. 2(b) and 2(d), the lattice spacings are 0.23 and 0.31 nm, corresponding to the $\text{Ag}(111)$ and $\text{CeO}_2(111)$, respectively [31–33]. The averaged size of Ag particles on Ag/SiC and $\text{Ag}/5\%\text{CeO}_2\text{-SiC}$

catalysts is statistically calculated to be 7.3 and 11.2 nm, respectively. The average particle size increases with the increase in modification amount of CeO_2 (Fig. S3, Table S3). In order to further clarify the distribution of CeO_2 and Ag on the SiC surface, element mapping tests were conducted on the $\text{Ag}/5\%\text{CeO}_2\text{-SiC}$ catalyst, as shown in Fig. 2(e-k). Fig. 2(e) shows the high-angle annular dark-field (HAADF) image of the catalyst. The yellow regions in Fig. 2(i) correspond to Ag particles, which align exactly with the bright spots in Fig. 2(e), indicating that the large spherical particles are indeed Ag. From Fig. 2(j), it is evident that the Ce element is uniformly distributed on the SiC surface, with no obvious large particle formation. These results demonstrate that Ag and CeO_2 have been successfully and uniformly dispersed on the SiC.

According to literature, the active component of ethylene epoxidation catalysts is metallic Ag [3]. Therefore, it is necessary to explore the valence state of Ag. UV-vis results show that the absorption values near 300 nm and 500 nm were significantly enhanced (Fig. S4). The absorption enhancement at 300 nm is attributed to the effects of CeO_2 , while the enhancement at 500 nm is attributed to Ag [34,35]. FTIR testing also revealed vibrational peaks corresponding to Ce-O and Si-C bonds in the catalyst (Fig. S5). These results demonstrate that the Ag component in the catalyst is metallic, providing the necessary conditions for activating oxygen. In addition, the valence states of elements on the

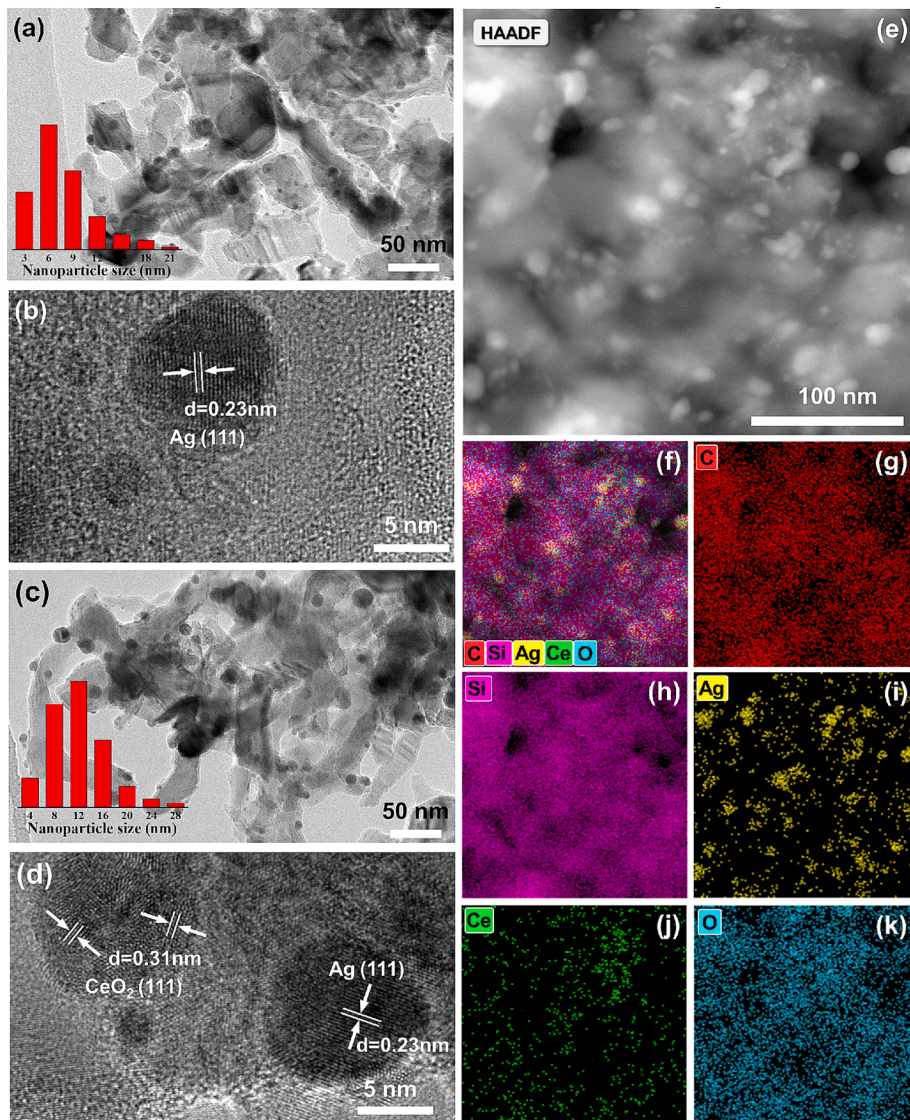


Fig. 2. TEM images of Ag/SiC (a,b) and $\text{Ag}/5\%\text{CeO}_2\text{-SiC}$ (c,d); HAADF image (e) and EDS mapping of $\text{Ag}/5\%\text{CeO}_2\text{-SiC}$ (f-k).

catalyst were further determined by XPS. The spectra of Ag 3d for the Ag/SiC and Ag/5%CeO₂-SiC catalysts are shown in Fig. 3(a). The binding energies at 368.2/368.3 eV and 374.2/374.3 eV correspond to the Ag 3d_{5/2} and Ag 3d_{3/2} spin-orbit doublets [10,36], respectively. The results indicate that the Ag of the Ag/CeO₂-SiC catalyst exists in a metallic state. Meanwhile, the peak near 450 nm in UV-vis testing is also related to Ag⁰ (Fig. S4) [37]. This provides additional evidence for the presence of metallic silver within the catalyst. Fig. 3(b) shows the Ce 3d spectrum of Ag/5%CeO₂-SiC catalyst. Referring to the work of Burroughs et al., the Ce 3d spectrum can be deconvoluted into 8 Gaussian peaks [38]. These peaks are labeled as the V series of Ce 3d_{5/2} and the U series of Ce 3d_{3/2}. Specifically, the peaks labeled as V, V'', V''', U, U'' and U''' correspond to Ce⁴⁺, while the peaks labeled as V' and U' correspond to the Ce³⁺ [33,39].

Usually, the formation process of Ce³⁺ is associated with the types of oxygen ions and the presence of oxygen vacancies (V_o) [40,41]. When oxygen spills from the lattice, it causes the Ce element to transition between Ce³⁺ and Ce⁴⁺ [28]. Furthermore, the Ce³⁺/(Ce³⁺ + Ce⁴⁺) ratio and the O/Ce ratio of the catalyst were calculated using formulas (4) and (5), respectively.

$$\text{Ce}^{3+}\% = \frac{S_U + S_V}{\sum (S_U + S_V)} \quad (4)$$

$$r_{\text{O}/\text{Ce}} = \frac{[\text{O}]}{[\text{Ce}^{4+}] + [\text{Ce}^{3+}]} = 2[\text{Ce}^{4+}] + 2/3[\text{Ce}^{3+}] \quad (5)$$

where Ce^{3+%} is the Ce³⁺/(Ce³⁺ + Ce⁴⁺) ratio, S_x is the XPS peak area corresponding to the x peak, r_{O/Ce} is the ratio of O element to Ce element, and [x] represents the proportion of x. The calculated Ce³⁺ content in

the Ag/5%CeO₂-SiC catalyst is 19.04 %. The r_{O/Ce} is 1.74, which is lower than the stoichiometric O/Ce ratio of CeO₂, indicating the presence of V_o. Fig. 3(c) shows the O 1 s spectrum of the catalysts. The O 1 s spectrum of the Ag/5%CeO₂-SiC catalyst can be deconvoluted into 3 peaks. The binding energies of 528.4, 530.9, and 531.4 eV are attributed to surface-lattice oxygen (O_{Lat}), surface-adsorbed oxygen (O_{Surf}), and hydroxyl or carbonate groups adsorbed on V_o, respectively [41,42]. However, for the O 1 s XPS spectrum of Ag/SiC, only one peak was deconvoluted, and this peak corresponds to surface-adsorbed oxygen. These oxygen atoms mainly originate from functional groups adsorbed on the SiC surface, such as SiO_xC_y, SiO₂, and -OH [43]. For the Ag/SiC catalyst, no lattice oxygen XPS peak appeared at ~ 528.4 eV. The comparison of O 1 s XPS spectra between Ag/SiC and Ag/5%CeO₂-SiC further confirms the presence of V_o on the Ag/5%CeO₂-SiC catalyst. In addition, after CeO₂ modification of Ag/SiC, the binding energies of C-Si in the C 1 s and Si-C in the Si 2p spectra both show a positive shift (Fig. S6). This indicates that an electron transfer occurs from SiC to CeO₂, consistent with previous studies [34]. This electron transfer may increase the proportion of Ce³⁺ species and promote oxygen vacancy formation.

Furthermore, singlet oxygen (¹O₂), superoxide radicals (•O₂) and V_o were determined through EPR testing by using 2,2,6,6-tetramethylpyridine (TEMP) and 5,5-dimethyl-1-pyrroline-N-oxide (DMPO) as trapping agents respectively. The EPR test results for the Ag/SiC and Ag/5%CeO₂-SiC catalytic systems at 30 min are shown in Fig. 4. Fig. 4(a) shows the characteristic peaks of the 1:1:1 triplet state, indicating the presence of ¹O₂ in the system [44]. Four strong peaks with an intensity ratio of 1:1:1:1 and two weak peaks are observed in Fig. 4(b), suggesting the generation of •O₂ in the system [45]. The above results indicate that both the Ag/SiC and Ag/5%CeO₂-SiC catalytic systems can produce ¹O₂.

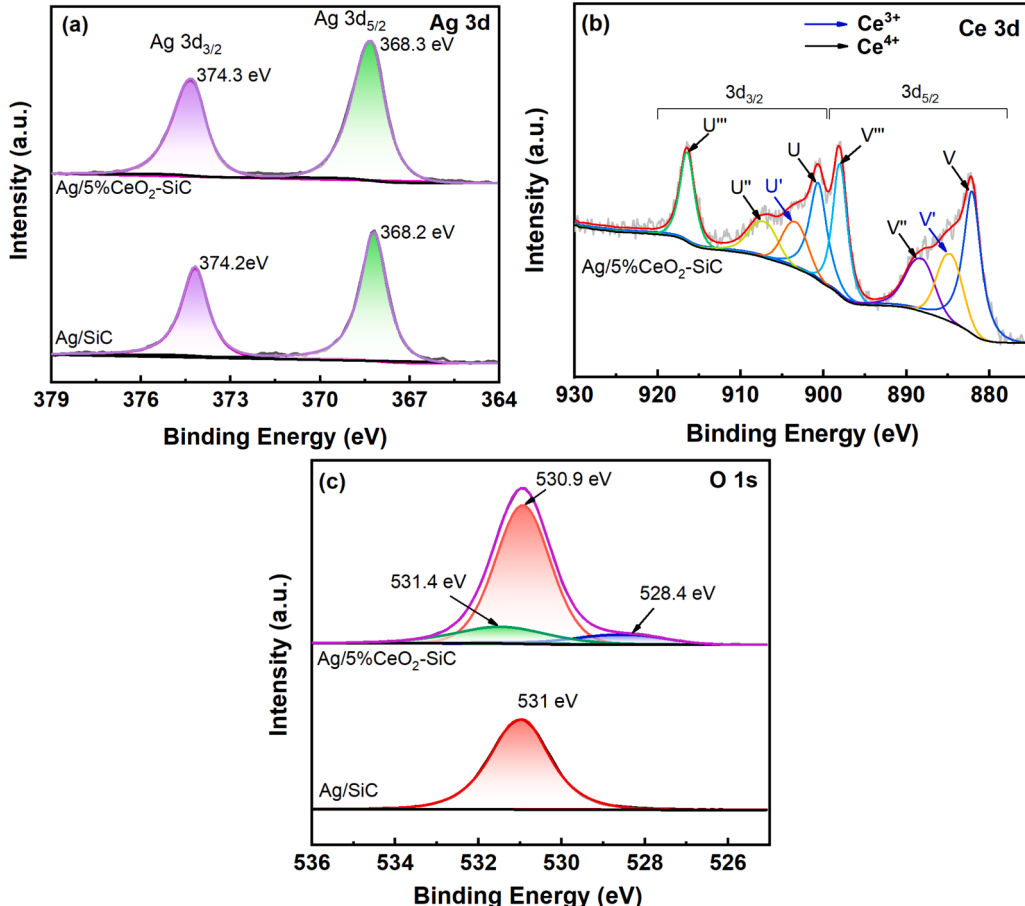


Fig. 3. XPS spectra of Ag 3d (a), O 1 s (b) and Ce 3d (c) in Ag/SiC and Ag/5%CeO₂-SiC catalysts.

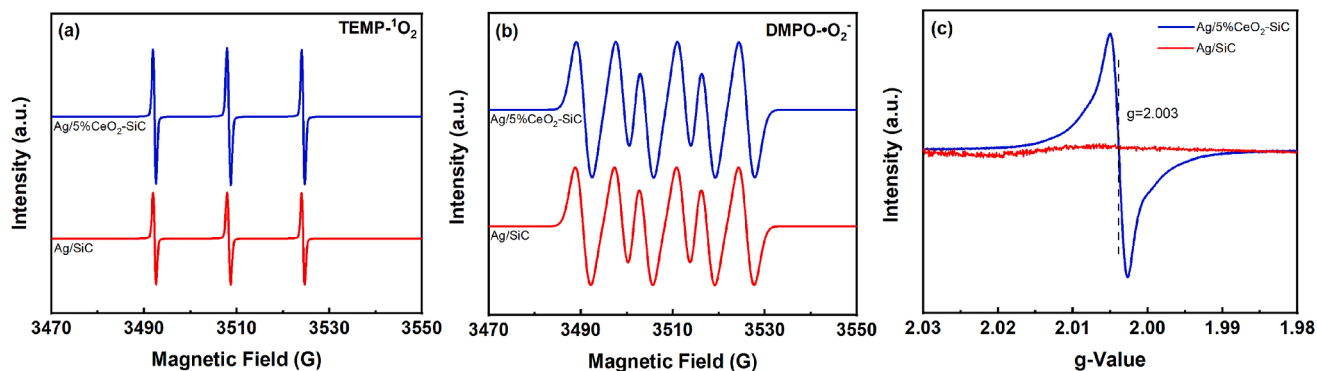


Fig. 4. EPR spectra of $^1\text{O}_2$ (a), $\bullet\text{O}_2^-$ (b) and V_0 (c) for Ag/SiC and Ag/5%CeO₂-SiC catalysts.

and $\bullet\text{O}_2^-$. From Fig. 4(c), No oxygen vacancy was detected in the Ag/SiC catalyst. While a typical g-value of 2.003 was observed in Ag/5%CeO₂-SiC, indicates the presence of V_0 in this system [46,47]. Subsequently, the quantitative analysis of V_0 and reactive oxygen species in Ag/SiC and CeO₂-modified Ag/SiC was conducted using Eaton's method [48], as shown in Table 1. The concentration of V_0 is 0 in Ag/SiC, but the concentrations of reactive oxygen species exceed 10^{11} spins/mm³. With an increase in the amount of CeO₂ modification, the concentrations of V_0 , $^1\text{O}_2$ and $\bullet\text{O}_2^-$ were significantly increased. This indicates that the modification with CeO₂ can introduce V_0 into the catalyst and promote the generation of reactive oxygen species [49].

The O₂ adsorption capacities of the Ag/SiC and CeO₂-modified Ag/SiC catalysts (CeO₂ contents: 3 %, 5 %, 7 %, and 10 %) further tested and found to be 29.12, 48.05, 55.27, 58.23 and 60.54 μmol/g (Table S4), respectively. The oxygen adsorption capacity of the catalyst is significantly enhanced by the CeO₂ modification. This further indicates that V_0 enhances the activation of oxygen. The Ag dispersion in the catalysts was determined by H₂ pulse adsorption. The Ag dispersion was measured to be 3.1 % in the Ag/SiC catalyst and 5.4 % in the Ag/5%CeO₂-SiC catalyst. Further calculations revealed that the O/Ag ratios for the two catalysts were 1.35 and 1.47, respectively. The O/Ag ratios in both catalysts exceeded 0.5, the stoichiometric ratio of O/Ag in Ag₂O, indicating the presence of oxygen spillover. The increase in the O/Ag ratio after CeO₂ modification indicates that V_0 has a promoting effect on oxygen spillover. In addition, the promoting effect of V_0 on the oxidation reaction was verified through controlled experiments of benzyl alcohol oxidation. The oxidation process was monitored using *In-situ* FTIR (Fig. S7). The results indicate that the CeO₂-modified catalyst can significantly promote the oxidation of benzyl alcohol.

The process of O₂ activation on these catalysts was further studied through *In-situ* Raman spectroscopy (Fig. 5). The oxygen species in the Raman spectra can be divided into three regions: atomic oxygen (240–500 cm⁻¹), hybrid oxygen (600–810 cm⁻¹), and molecular oxygen (850–1150 cm⁻¹) [50]. From Fig. 5, both Ag/SiC and Ag/5%CeO₂-SiC catalysts exhibited multiple Raman peaks, which were attributed to various binding modes of oxygen on the catalyst surface. Specifically, the peaks observed at 317 and 311 cm⁻¹ can correspond to Ag₃-O [51], while those at 443 and 448 cm⁻¹ can correspond to O-Ag-O [51,52]. The peaks located at 785, 795, 763, and 787 cm⁻¹ are typically associated

with surface or subsurface adsorbed hybrid oxygen species, such as Ag₄O₂ and Ag-O_{surface} [51,53]. The features at 865 and 950 cm⁻¹ can be assigned to surface Ag-O [53,54]. The peak near 1060 cm⁻¹ can be attributed to the superoxide Ag-O²⁻ [51,53,54]. When the temperature exceeds 150 °C, the peak at 795 cm⁻¹ in Fig. 5(a) undergoes a red shift, which is related to the exchange of surface oxygen with gas-phase O₂ molecules on the surface [20]. Similarly, the peak located at 787 cm⁻¹ in Fig. 5(b) also exhibits a red shift, indicating that Ag can effectively activate oxygen. It was reported that the Raman peak corresponding to the F_{2g} symmetric vibration mode in CeO₂ was located at 460 cm⁻¹ [55]. However, the Raman peak of CeO₂ in this work is located at 448 cm⁻¹. This redshift of the peak may suggest the existence of V_0 defects in CeO₂ [56]. When the temperature exceeds 100 °C, the peak intensity at 448 cm⁻¹ in Fig. 5(b) significantly increases. Meanwhile, the peak intensity near 787 cm⁻¹ is significantly reduced compared to Fig. 5(a). This change may be caused by oxygen vacancies present in CeO₂. After oxygen is activated on the surface of Ag, V_0 promotes the migration of reactive oxygen species to the surface of CeO₂.

It is generally recognized that the ethylene epoxidation process predominantly occurs on the Ag surface. In this reaction, active oxygen species activated on Ag can react with ethylene to form an oxametallacycle intermediate on the Ag surface. Subsequently, the oxametallacycle intermediate undergoes isomerization to form EO [11,57–59]. However, this work suggests another possible route. Ethylene is adsorbed and activated on the SiC surface. The oxygen species, activated on Ag surface, spills over to the SiC surface, and then react with the adsorbed ethylene. The adsorption of ethylene on the SiC was verified using an adsorption instrument. The TPD curves of different samples after adsorbing ethylene were measured, as shown in Fig. 6. The TPD results show a similar desorption peak for SiC, Ag/SiC, and Ag/5%CeO₂-SiC in the range of 504–507 °C. The desorption peak can be ascribed to the desorption of ethylene chemisorbed on SiC. However, the desorption peak was not observed in CeO₂, indicating that the CeO₂ surface did not adsorb ethylene. When the modification amount was too high, the surface of the SiC became increasingly covered by CeO₂, hindering the adsorption of ethylene on the SiC surface. Therefore, the reaction performance decreased at high CeO₂ modification levels (Fig. 1).

To further verify the adsorption of ethylene on SiC surface, the adsorption energy of ethylene on the surfaces of various components was calculated by DFT. The calculated adsorption energies of ethylene on Si-terminated SiC and C-terminated SiC were -3.96 and -3.87 eV (Fig. S8, Table S5), respectively, indicating a strong adsorption interaction between ethylene and the SiC surface. To more realistically simulate the actual situation, a model where SiC, Ag and CeO₂ coexist was built for the calculation. The adsorption energies of ethylene on the surfaces of SiC, Ag, and CeO₂ are -3.25, -0.11, and -0.10 eV (Fig. S9, Table S5), respectively. Compared with the C=C bond length of 1.33 Å in gaseous ethylene molecules [60], it significantly increases to 1.575 Å after adsorption on the SiC surface. Theoretical calculations further

Table 1
Active oxygen concentration in Ag/SiC and different CeO₂-modified catalysts.

Ag Catalysts	Concentration (spins/mm ³)		
	$^1\text{O}_2$	$\bullet\text{O}_2^-$	V_0
Ag/SiC	1.49×10^{11}	1.43×10^{12}	0
Ag/3%CeO ₂ -SiC	1.96×10^{11}	1.51×10^{12}	9.28×10^{12}
Ag/5%CeO ₂ -SiC	2.11×10^{11}	1.69×10^{12}	1.45×10^{13}
Ag/7%CeO ₂ -SiC	2.87×10^{11}	3.23×10^{12}	5.74×10^{13}
Ag/10%CeO ₂ -SiC	4.25×10^{11}	6.57×10^{12}	8.13×10^{13}

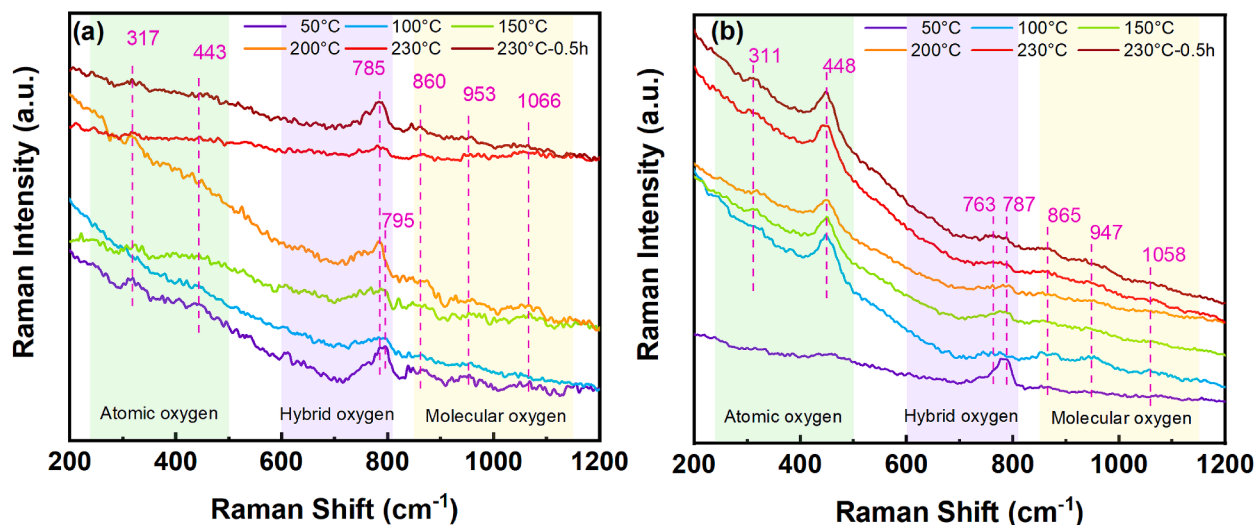


Fig. 5. *In-situ* Raman spectra of Ag/SiC (a) and Ag/5%CeO₂-SiC (b) catalysts under O₂ atmosphere.

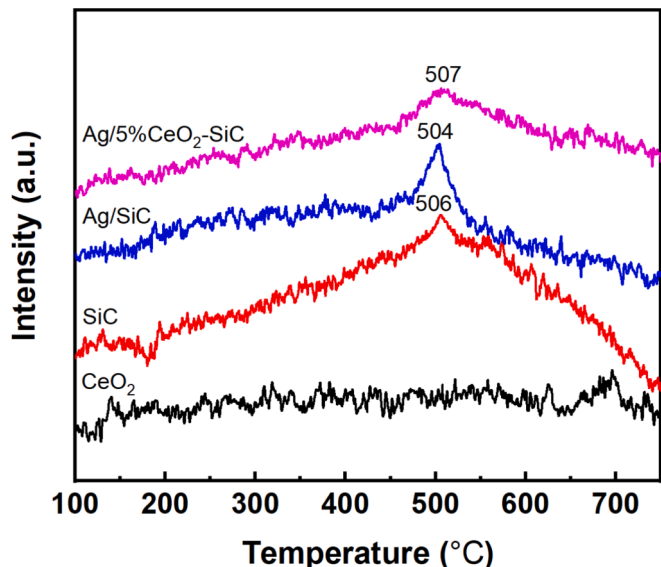


Fig. 6. TPD results of ethylene on different samples.

indicate that ethylene molecules are preferentially adsorbed and activated on the SiC surface, consistent with the results of the TPD results. In addition, previous reports have also indicated that ethylene was adsorbed on SiC [60].

Based on the experimental and calculated results, a possible reaction route was proposed to understand the ethylene epoxidation on SiC supported Ag catalysts. Firstly, O₂ is activated on the Ag surface and subsequently transformed into ¹O₂ and •O₂⁻, while ethylene is activated on the surface of SiC. Next, the ¹O₂ and •O₂⁻ undergo a migration to the SiC surface and react with the activated ethylene. The V_o in CeO₂ can enhance the catalytic activity by promoting the migration of oxygen species. The route also produces by-products of excessive oxidation, including water and CO₂. This route differs from the commonly recognized viewpoint that oxametallacycle intermediates react on the Ag surface.

4. Conclusion

In summary, we employed CeO₂-modified SiC as the support and prepared a low Ag-loaded (15 wt%) catalyst, Ag/5%CeO₂-SiC for the

ethylene epoxidation. The catalyst exhibited good activity and selectivity. At 230 °C, the reaction showed 5.4 % conversion, 74.3 % ethylene oxide selectivity, and a space-time yield of 66 kg/(m³·h). The experimental and computational results suggested a different activation and reaction route for ethylene epoxidation over the Ag catalyst supported on SiC. ¹O₂ and •O₂⁻ were formed on the Ag surface and then migrated to the SiC surface, where they react with ethylene adsorbed on the SiC. The V_o in CeO₂ can promote the spillover of these oxygen species, ultimately enhancing the reaction performance. This work provides new perspectives for a deeper understanding of ethylene epoxidation reactions and contributes to the development of catalysts for epoxidation.

CRediT authorship contribution statement

Xiang Li: Writing – original draft, Investigation, Funding acquisition, Formal analysis, Data curation. **Jixiao Zhao:** Supervision, Project administration, Methodology, Formal analysis. **Zhenni Wei:** Validation, Methodology, Formal analysis, Data curation. **Xiaofei Liu:** Methodology, Formal analysis. **Xin Huang:** Methodology, Data curation. **Guoqiang Zhang:** Data curation. **Yu Liu:** Methodology, Data curation. **Zhifeng Jiao:** Writing – review & editing, Supervision, Project administration, Methodology. **Xiangyun Guo:** Writing – review & editing, Supervision, Methodology, Funding acquisition, Conceptualization.

Declaration of competing interest

The authors declare that they have no known competing financial interests or personal relationships that could have appeared to influence the work reported in this paper.

Acknowledgements

This work was supported by a project from CNPC-CZU Innovation Alliance (2021DQ06) and Postgraduate Research & Practice Innovation Program of Jiangsu Province (KYCX23_3024).

Appendix A. Supplementary data

Supplementary data to this article can be found online at <https://doi.org/10.1016/j.fuel.2025.135496>.

Data availability

Data will be made available on request.

References

- [1] Van Hoof AJF, Hermans EAR, Van Bavel AP, Friedrich H, Hensen EJM. Structure sensitivity of silver-catalyzed ethylene epoxidation. *ACS Catal* 2019;9:9829–39. <https://doi.org/10.1021/acscatal.9b02720>.
- [2] Fazeli A, Naseri A, Eslamjamal F. Kinetic models of ethylene oxide production on Ag catalysts: A review. *Kinet Catal* 2020;61:603–12. <https://doi.org/10.1134/S0023158420040059>.
- [3] Ozbek MO, Onal I, van Santen RA. Why silver is the unique catalyst for ethylene epoxidation. *J Catal* 2011;284:230–5. <https://doi.org/10.1016/j.jcat.2011.08.004>.
- [4] Van Santen RA, Kuipers HPCE. The mechanism of ethylene epoxidation. *Adv Catal* 1987;35:265–321. [https://doi.org/10.1016/S0360-0564\(08\)60095-4](https://doi.org/10.1016/S0360-0564(08)60095-4).
- [5] Mavrikakis M, Doren DJ, Bartea MA. Density functional theory calculations for simple oxometallacycles: Trends across the periodic table. *J Phys Chem B* 1998; 102:394–9. <https://doi.org/10.1021/jp971450p>.
- [6] Reuter K, Scheffler M. Oxide formation at the surface of late 4d transition metals: insights from first-principles atomistic thermodynamics. *Appl Phys A* 2004;78: 793–8. <https://doi.org/10.1007/s00339-003-2433-9>.
- [7] Pinaeva LG, Noskov AS. Prospects for the development of ethylene oxide production catalysts and processes (Review). *Pet Chem* 2020;60:1191–206. <https://doi.org/10.1134/S096554412011016X>.
- [8] Ozbek MO, Santen R. The mechanism of ethylene epoxidation catalysis. *Catal Lett* 2013;143:131–41. <https://doi.org/10.1007/s10562-012-0957-3>.
- [9] Santos VP, Plauck A, Gold J, Majumdar P, McDonagh MH, Calverley T. The complex chlorination effects on high selectivity industrial EO catalysts: dynamic interplay between catalyst composition and process conditions. *ACS Catal* 2024;14: 10839–52. <https://doi.org/10.1021/acscatal.4c01764>.
- [10] Dia W, DiGiulio CD, Schaal MT, Ma S, Monnier JR. An investigation on the role of Re as a promoter in $\text{Ag}-\text{Cs}-\text{Re}/\alpha-\text{Al}_2\text{O}_3$ high-selectivity, ethylene epoxidation catalysts. *J Catal* 2015;322:14–23. <https://doi.org/10.1016/j.jcat.2014.11.007>.
- [11] Pu T, Setiawan A, Foucher AC, Guo M, Jehng J-M, Zhu M, et al. Revealing the Nature of Active Oxygen Species and Reaction Mechanism of Ethylene Epoxidation by Supported $\text{Ag}/\alpha-\text{Al}_2\text{O}_3$ Catalysts. *ACS Catal* 2024;14:406–17. <https://doi.org/10.1021/acscatal.3e04361>.
- [12] Yang H, Li G, Liu Q, Cheng H, Wang X, Cheng J, et al. Tailoring the electronic metal-support interactions in supported silver catalysts through Al modification for efficient ethylene epoxidation. *Angew Chem Int Ed* 2024;63:e202400627. <https://doi.org/10.1002/anie.202400627>.
- [13] Wen Q, Xu H, Nan Y, Xie Y, Cheng D. Design of CuCs-doped Ag-based catalyst for ethylene epoxidation. *Chin J Chem Phys* 2022;35:589–99. <https://doi.org/10.1063/1674-0068/cjcp2111246>.
- [14] Van Hoof AJF, Van Der Poll RCJ, Friedrich H, Hensen EJM. Dynamics of silver particles during ethylene epoxidation. *Appl Catal, B* 2020;272:118983. <https://doi.org/10.1016/j.apcatb.2020.118983>.
- [15] Ren D, Cheng G, Li J, Li J, Dai W, Sun X, et al. Effect of rhodium loading sequence on selectivity of $\text{Ag}-\text{Cs}$ catalyst for ethylene epoxidation. *Catal Lett* 2017;147: 2920–8. <https://doi.org/10.1007/s10562-017-2211-5>.
- [16] Rojuechaei S, Chavadej S, Schwank JW, Meeyou V. Catalytic activity of ethylene oxidation over Au, Ag and Au–Ag catalysts: Support effect. *Catal Commun* 2007;8: 57–64. <https://doi.org/10.1016/j.catcom.2006.05.029>.
- [17] Li H, Cao A, Nørskov JK. Understanding trends in ethylene epoxidation on group IB metals. *ACS Catal* 2021;11:12052–7. <https://doi.org/10.1021/acscatal.1c03094>.
- [18] Ramirez A, Hueso JL, Suarez H, Mallada R, Ibarra A, Irusta S, et al. A nanoarchitecture based on silver and copper oxide with an exceptional response in the chlorine-promoted epoxidation of ethylene. *Angew Chem Int Ed* 2016;55: 11158–61. <https://doi.org/10.1002/anie.201603886>.
- [19] Marek EJ, Gabra S, Dennis JS, Scott SA. High selectivity epoxidation of ethylene in chemical looping setup. *Appl Catal, B* 2020;262:118216. <https://doi.org/10.1016/j.apcatb.2019.118216>.
- [20] Pu T, Tian H, Ford ME, Rangarajan S, Wachs IE. Overview of Selective Oxidation of Ethylene to Ethylene Oxide by Ag Catalysts. *ACS Catal* 2019;9:10727–50. <https://doi.org/10.1021/acscatal.9b03443>.
- [21] Ortega-Trigueros A, Narciso J, Caccia M. Synthesis of high-surface area mesoporous SiC with hierarchical porosity for use as catalyst support. *J Am Ceram Soc* 2020;103:5966–77. <https://doi.org/10.1111/jace.17285>.
- [22] Tuci G, Liu Y, Rossin A, Guo X, Pham C, Giambastiani G, et al. Porous silicon carbide (SiC): A chance for improving catalysts or just another active-phase carrier? *Chem Rev* 2021;121:10559–665. <https://doi.org/10.1021/acs.chemrev.1c00269>.
- [23] Hao C-H, Guo X-N, Sankar M, Yang H, Ma B, Zhang Y-F, et al. Synergistic effect of segregated Pd and Au nanoparticles on semiconducting SiC for efficient photocatalytic hydrogenation of nitroarenes. *ACS Appl Mater Interfaces* 2018;10: 23029–36. <https://doi.org/10.1021/acsm.8b04044>.
- [24] Jiao Z-F, Zhao J-X, Guo X-N, Tong X-L, Zhang B, Jin G-Q, et al. Turning the product selectivity of nitrile hydrogenation from primary to secondary amines by precise modification of Pd/SiC catalysts using NiO nanodots. *Catal Sci Technol* 2019;9: 2266. <https://doi.org/10.1039/c9cy00353c>.
- [25] Li L, Jiao Z-F, Zhao J-X, Yao D, Li X, Guo X-Y. Boosting the selectivity of Pt catalysts for cinnamaldehyde hydrogenation to cinnamylalcohol by surface oxidation of SiC support. *J Catal* 2023;425:314–21. <https://doi.org/10.1016/j.jcat.2023.06.018>.
- [26] Zheng Z-Y, Jiao Z-F, Zhao J-X, Liu X-C, Song C-D, Li J-H, et al. Selective adsorption of SiC quantum dots to C=O bond promoting the catalytic hydrogenation of cinnamaldehyde. *Chem Eng J* 2025;503:158727. <https://doi.org/10.1016/j.cej.2024.158727>.
- [27] Li X, Jiao Z-F, Zhao J-X, Xu T-Y, Guo X-Y. Catalytic performances of Ag/SiC catalysts for styrene epoxidation in O_2 atmosphere. *Appl Catal, A* 2024;688: 120004. <https://doi.org/10.1016/j.apcata.2024.120004>.
- [28] Li R, Wen C, Yan K, Liu T, Zhang B, Xu M, et al. The water splitting cycle for hydrogen production at photo-induced oxygen vacancies using solar energy: experiments and DFT calculation on pure and metal-doped CeO_2 . *J Mater Chem A* 2023;11:7128–41. <https://doi.org/10.1039/D2TA08833A>.
- [29] Liu J, Wang H, Zhang W, Gao J, Yu Q, Ke J, et al. Boosting the performance of Co-doped CeO_2 catalyst in the catalytic oxidation of toluene by modulating oxygen vacancies. *Fuel* 2023;349:128657. <https://doi.org/10.1016/j.fuel.2023.128657>.
- [30] Christopher P, Linic S. Engineering Selectivity in Heterogeneous Catalysis: Ag Nanowires as Selective Ethylene Epoxidation Catalysts. *J Am Chem Soc* 2008;130: 11264–5. <https://doi.org/10.1021/ja803818k>.
- [31] Wang Y, Bi F, Wang Y, Jia M, Tao X, Jin Y, et al. MOF-derived CeO_2 supported Ag catalysts for toluene oxidation: The effect of synthesis method. *Mol Catal* 2021; 515:111922. <https://doi.org/10.1016/j.mcat.2021.111922>.
- [32] Li X, Jiao Z, Zhao J, Wei Z, Liu Y, Guo X. Catalytic performances of Ag/SiC and Ag/ Al_2O_3 -SiC catalysts for ethylene epoxidation. *Journal of Changzhou University (Natural Science Edition)* 2024;36:85–92. <https://doi.org/10.3969/j.issn.2095-0411.2024.02.009>.
- [33] Liang X, Wang P, Gao Y, Huang H, Tong F, Zhang Q, et al. Design and synthesis of porous M-ZnO/ CeO_2 microspheres as efficient plasmonic photocatalysts for nonpolar gaseous molecules oxidation: Insight into the role of oxygen vacancy defects and M=Ag, Au nanoparticles. *Appl Catal, B* 2020;260:118151. <https://doi.org/10.1016/j.apcatb.2019.118151>.
- [34] Gao J, Tang L, Shen Z, Dong Y, Wang Z, Lyu J, et al. Coupling of SiC and CeO_2 nanosheets to enhance solar energy utilization and optimize catalytic ozonation. *Appl Catal, B* 2022;317:121697. <https://doi.org/10.1016/j.apcatb.2022.121697>.
- [35] Gannoruwa A, Ariyasinghe B, Bandara J. The mechanism and material aspects of a novel $\text{Ag}_2\text{O}/\text{TiO}_2$ photocatalyst active in infrared radiation for water splitting. *Catal Sci Technol* 2016;6:479–87. <https://doi.org/10.1039/C5CY01002K>.
- [36] Li R, Xu X, Zhu B, Li X-Y, Ning Y, Mu R, et al. In situ identification of the metallic state of Ag nanoclusters in oxidative dispersion. *Nat Commun* 2021;12:1406. <https://doi.org/10.1038/s41388-021-0552-2>.
- [37] Wang F, Ma J, He G, Chen M, Zhang C, He H. Nanosize effect of Al_2O_3 in Ag/ Al_2O_3 catalyst for the selective catalytic oxidation of ammonia. *ACS Catal* 2018;8: 2670–82. <https://doi.org/10.1021/acscatal.7b03799>.
- [38] Burroughs P, Hamnett A, Orchard AF, Thornton G. Satellite structure in the X-ray photoelectron spectra of some binary and mixed oxides of lanthanum and cerium. *J Chem Soc, Dalton Trans* 1976;1686. <https://doi.org/10.1039/dt9760001686>.
- [39] Wang X, Wang Y, Robinson B, Wang Q, Hu J. Ethane oxidative dehydrogenation by CO_2 over stable CsRu/CeO_2 catalyst. *J Catal* 2022;413:138–49. <https://doi.org/10.1016/j.jcat.2022.06.021>.
- [40] Wu S, Yang Y, Lu C, Ma Y, Yuan S, Qian G. Soot oxidation over CeO_2 or Ag/ CeO_2 : Influences of bulk oxygen vacancies and surface oxygen vacancies on activity and stability of the catalyst. *Eur J Inorg Chem* 2018;2018:2944–51. <https://doi.org/10.1002/ejic.201800423>.
- [41] Mi R, Li D, Hu Z, Yang RT. Morphology effects of CeO_2 nanomaterials on the catalytic combustion of toluene: A combined kinetics and diffuse reflectance infrared Fourier transform spectroscopy study. *ACS Catal* 2021;11:7876–89. <https://doi.org/10.1021/acscatal.1c01981>.
- [42] Torrente-Murcia L, Gilbank A, Puertas B, Garcia T, Solsona B, Chadwick D. Shape-dependency activity of nanostructured CeO_2 in the total oxidation of polycyclic aromatic hydrocarbons. *Appl Catal, B* 2013;132–133:116–22. <https://doi.org/10.1016/j.apcatb.2012.10.030>.
- [43] Carrero CA, Burt SP, Huang F, Venegas JM, Love AM, Mueller P, et al. Supported two- and three-dimensional vanadium oxide species on the surface of β -SiC. *Catal Sci Technol* 2017;7:3707–14. <https://doi.org/10.1039/C7CY01036B>.
- [44] Li H, Zou Y, Jiang J. Synthesis of Ag@CuO nanohybrids and their photo-enhanced bactericidal effect through concerted Ag ion release and reactive oxygen species generation. *Dalton Trans* 2020;49:9274–81. <https://doi.org/10.1039/DOT01816C>.
- [45] Cao L, Yang C, Zhang B, Lv K, Li M, Deng K. Synergistic photocatalytic performance of cobalt tetra-(2-hydroxymethyl-1,4-dithiin) porphyrazine loaded on zinc oxide nanoparticles. *J Hazard Mater* 2018;359:388–95. <https://doi.org/10.1016/j.jhazmat.2018.07.074>.
- [46] Zhao S, Kang D, Liu Y, Wen Y, Xie Y, Yi H, et al. Spontaneous formation of asymmetric oxygen vacancies in transition-metal-doped CeO_2 nanorods with improved activity for carbonyl sulfide hydrolysis. *ACS Catal* 2020;10:11739–50. <https://doi.org/10.1021/acscatal.0c02832>.
- [47] Xiao Y, Tian S, Wang D, Wu J, Jia T, Liu Q, et al. $\text{CeO}_2/\text{BiOIO}_3$ heterojunction with oxygen vacancies and Ce⁴⁺/Ce³⁺ redox centers synergistically enhanced photocatalytic removal heavy metal. *Appl Surf Sci* 2020;530:147116. <https://doi.org/10.1016/j.apsusc.2020.147116>.
- [48] Eaton GR, Eaton SS, Barr DP, Weber RT. Quantitative EPR. Springer, New York, 2010, <https://link.springer.com/book/10.1007/978-3-211-92948-3>.
- [49] He H, Lin X, Li S, Wu Z, Gao J, Wu J, et al. The key surface species and oxygen vacancies in $\text{MnO}_x(0.4)-\text{CeO}_2$ toward repeated soot oxidation. *Appl Catal, B* 2018; 223:134–42. <https://doi.org/10.1016/j.apcatb.2017.08.084>.
- [50] Tang Z, Chen T, Liu K, Du H, Podkolzin SG. Atomic, molecular and hybrid oxygen structures on silver. *Langmuir* 2021;37:11603–10. <https://doi.org/10.1021/acs.langmuir.1c01941>.
- [51] Pu T, Setiawan A, Lis BM, Zhu M, Ford ME, Rangarajan S, et al. Nature and reactivity of oxygen species on/in silver catalysts during ethylene oxidation. *ACS Catal* 2022;12:4375–81. <https://doi.org/10.1021/acscatal.1c05939>.

- [52] Guo J, Ghimire G, Zhou J, Yu L, Wang Z, Chang S, et al. Potential controlled redox cycling of 4-aminothiophenol by coupling plasmon mediated chemical reaction with electrochemical reaction. *J Catal* 2023;418:256–62. <https://doi.org/10.1016/j.jcat.2023.01.018>.
- [53] Liu C, Wijewardena DP, Sviripa A, Sampath A, Flaherty DW, Paolucci C. Computational and experimental insights into reactive forms of oxygen species on dynamic Ag surfaces under ethylene epoxidation conditions. *J Catal* 2022;405: 445–61. <https://doi.org/10.1016/j.jcat.2021.11.031>.
- [54] Wang C-B, Deo G, Wachs IE. Interaction of polycrystalline silver with oxygen, water, carbon dioxide, ethylene, and methanol: In situ Raman and catalytic studies. *J Phys Chem B* 1999;103:5645–56. <https://doi.org/10.1021/jp984363l>.
- [55] Li Z, Yang W, Xie L, Li Y, Liu Y, Sun Y, et al. Prominent role of oxygen vacancy for superoxide radical and hydroxyl radical formation to promote electro-Fenton like reaction by W-doped CeO₂ composites. *Appl Surf Sci* 2021;549:149262. <https://doi.org/10.1016/j.apsusc.2021.149262>.
- [56] Choudhury B, Chetri P, Choudhury A. Oxygen defects and formation of Ce³⁺ affecting the photocatalytic performance of CeO₂ nanoparticles. *RSC Adv* 2014;4: 4663–71. <https://doi.org/10.1039/C3RA44603D>.
- [57] Chen BWJ, Wang B, Sullivan MB, Borgna A, Zhang J. Unraveling the Synergistic Effect of Re and Cs Promoters on Ethylene Epoxidation over Silver Catalysts with Machine Learning-Accelerated First-Principles Simulations. *ACS Catal* 2022;12: 2540–51. <https://doi.org/10.1021/acscatal.1c05419>.
- [58] Yu Z, Zhu L, Xu H, Cheng D. Selective enhancement of ethylene epoxidation via directing reaction pathways over Ag Single-atom catalyst. *Ind Eng Chem Res* 2024; 63:3044–56. <https://doi.org/10.1021/acs.iecr.3c04600>.
- [59] Iyer KR, Bhan A. Particle size dependence of ethylene epoxidation rates on Ag/ α -Al₂O₃ catalysts: Why particle size distributions matter. *J Catal* 2023;420:99–109. <https://doi.org/10.1016/j.jcat.2023.02.008>.
- [60] Pollmann J, Peng X, Wieferink J, Krüger P. Adsorption of hydrogen and hydrocarbon molecules on SiC(001). *Surf Sci Rep* 2014;69:55–104. <https://doi.org/10.1016/j.surfrept.2014.04.001>.